European Journal of Vascular and Endovascular Surgery 44 (2012) 475–481

Contents lists available at SciVerse ScienceDirect

European Journal of Vascular and Endovascular Surgery

journal homepage: www.ejves.com

In Vivo Assessment of Murine Elastase-induced Abdominal Aortic Aneurysm with High Resolution Magnetic Resonance Imaging

M.A. Bartoli [a,b,*], F. Kober [a], P. Cozzone [a], R.W. Thompson [d], M.C. Alessi [c], M. Bernard [a]

[a] *Aix-Marseille université, CNRS, CRMBM UMR 7339, 13385 Marseille cedex 5, France*
[b] *Aix-Marseille université, APHM, Hôpital de la Timone, Service de Chirurgie Vasculaire, 13385 Marseille cedex 5, France*
[c] *Aix-Marseille université, INSERM, NORT UMR_S 1062, 13385 Marseille cedex 5, France*
[d] *Department of Surgery (Section of Vascular Surgery), Washington University School of Medicine, St. Louis, MO, USA*

WHAT THIS PAPER ADDS?

- Aortic abdominal aneurysm mouse models are a valuable tool to study the pathogenesis of this condition. Recently, it has been shown that AAAs developed in the murine elastase-induced model are measurable with ultrasound. In this study we demonstrated the feasibility of aortic measurement with MRI in this particular model. Because MRI may provide cellular and biochemical information about the aortic wall, the development of an aneurysm follow-up model with MRI could provide new insights concerning risk factors for rupture or help to predict rapid evolution of AAAs still under surveillance.

ARTICLE INFO

Article history:
Received 1 March 2012
Accepted 1 August 2012
Available online 30 August 2012

Keywords:
High resolution MRI
Murine elastase-induced abdominal aortic aneurysm
AAA

ABSTRACT

Objectives: There are, to date, no published non-invasive or longitudinal studies performed in mice to measure aortic diameter and wall thickness in an elastase-induced abdominal aortic aneurysm. This MRI study at 11.75 T aimed at evaluating the reliability of longitudinal *in vivo* aortic diameter and wall thickness measurements in this particular model.
Methods: Adult male C57BL/6 mice underwent transient elastase or heat-inactivated elastase perfusion (controls). Aortic dilatation was measured before, during and immediately after elastase perfusion, and again 14 days after, with a calibrated ocular grid. MRI was performed just before initial surgery and at day 14 before harvest using an 11.75 T MR microscopy imager.
Results: Aortic diameter was significantly greater in elastase-perfused mice compared to controls as measured by optic grid (1.150 ± 0.153 mm vs 0.939 ± 0.07 mm, $P = 0.038$) and according to MRI measurement of the outer diameter on spin echo images (1.203 ± 0.105 mm vs 1070 ± 0.048 mm, $P = 0.0067$). Aortic wall thickness was found to be significantly increased in elastase-perfused mice at day 14.
Conclusions: This study demonstrates in the mouse elastase-induced aneurysm model that characterization of aneurysm development by its inner and outer vessel diameter and vessel wall thickness can be carried out longitudinally using high resolution MRI without significant mortality.

Introduction

Abdominal aortic aneurysm (AAA) is a common and potentially life-threatening condition associated with advanced age, cigarette smoking, atherosclerosis, and an inherited predisposition. Several animal models have been developed to determine the mechanism of AAA formation.[1] The most commonly used mouse models of AAA are produced by calcium chloride,[2] angiotensin II (AngII)[3] or elastase.[4] The infusion of AngII into either fat fed, LDL receptor −/− or apolipoprotein E-deficient mice (ApoE-KO) leads to the production of a suprarenal aneurysm. Surprisingly, in this model, medial early events are accumulation of macrophages and dissection, a different aortic

* Corresponding author. M.A. Bartoli, Faculté de médecine de Marseille, UFR médecine site TIMONE, CRMBM, CNRS UMR 7339, Boulevard Jean Moulin, 13385 Marseille cedex 5, France. Tel.: +33 491 385 762; fax: +33 491 384 370.
E-mail address: michel.bartoli@ap-hm.fr (M.A. Bartoli).

1078-5884/$ – see front matter
http://dx.doi.org/10.1016/j.ejvs.2012.08.002

pathological entity as supposed to aneurysm.[5] Despite a very reproducible localization of the AAA in the suprarenal region of the aorta during AngII infusion, it has been observed that specific experimental conditions can generate AAAs that are grossly variable in morphologic appearance. However, these variations were not easily reflected by any measurements such as changes in vessel size. Therefore, a classification system for different forms of AAAs has been established.[6] However, this classification might be difficult to assess with current MRI or duplex techniques. In the second model, peri-aortic incubation of calcium chloride promoted arterial wall thickening. This model led to the development of luminal dilatation, but without the preceding mechanical effects that are noted in the elastase perfusion model.[2] The elastase perfusion model was initially performed in rats and later transferred to mice.[4,7] The adaptation of the elastase perfusion model to mice has brought the important advantage of allowing studies in genetically modified strains, and therefore has led to a more sophisticated definition of the underlying mechanisms. On the other hand, this adaptation implies working on much smaller aortic diameters. The elastase perfusion model in mice involves transient elastase-induced aortic injury resulting in only mild to moderate immediate aortic dilatation within 14 days of surgery. This reproduces many of the critical features of human AAAs, including transmural infiltration of the aortic wall by mononuclear phagocytes, increased local production of MMPs, and progressive degradation of aortic wall matrix proteins.[8] MRI is an ideal tool for vascular research, because it can generate high-resolution images across many time-points and assess the vascular wall biology. Previously published studies have already used MRI in mouse models of atherosclerosis[9,10] and in other models of aortic aneurysms.[11,12] However, and to the best of our knowledge, this is the first time that MRI has been used to assess the aorta in the elastase perfusion model. Indeed, aneurysm size in the elastase model is small (diameters around 1.3 mm) compared for example to the aneurysm created in the ApoE angiotensin model (diameters around 2.5 mm). These measurements required high spatial resolutions and have been possible with the use of high field MRI (11.75 T), which is an innovative tool in small animal cardiovascular research. The aim of this study was to demonstrate the feasibility and the reliability of *in vivo* MRI measurements of aortic morphology in the elastase perfusion model in C57Bl/6 mice in comparison to the reference method by microscope grid measurements. As a longer-term goal, this study may serve as a basis for multiparametric and molecular MR imaging,[11,13] and may provide helpful information for future clinical applications.

Materials & Methods

Elastase perfusion model of AAA

Eighteen adult male 8–12 week old C57BL/6J mice (HARLAN, Indianapolis, IN, USA) were used. Within this very common age range, variations in size, weight and aortic diameter are known to be small.[14,15] Animals were cared for and used according to a protocol approved by the committee on animal ethics at the Université de la Méditerranée, and in accordance with the European convention for the protection of vertebrate animals used for experimental purposes and institutional guidelines n° 86/609/CEE November 24, 1986. The mice were randomly assigned to two groups, nine undergoing elastase perfusion and the remaining nine undergoing heat-inactivated elastase (HIE) perfusion for control. They underwent transient perfusion of the abdominal aorta to induce AAAs, as described previously.[4] The mice were anesthetized, and a laparotomy was performed with the assistance of an operating stereo microscope (Leica). The infrarenal abdominal aorta was isolated, and the pre-perfusion aortic diameter was measured with a calibrated ocular grid. The isolated aortic lumen was perfused for 5 min at 100 mmHg (1 mmHg _ 133 Pa) with a saline solution containing type 1 porcine pancreatic elastase in 9 mice (0.1455 units/ml; Sigma, St. Louis, MO, USA). The elastase dose for inducing AAAs with confidence and without aortic dystrophy was determined in preparative experiments carried out on 49 mice: HIE group ($n = 9$), 0.1164 units/ml ($n = 10$), 0.1455 units/ml ($n = 11$), 0.1746 units/ml ($n = 12$) and 0.2328 units/ml ($n = 7$). During this initial phase mouse mortality was measured. The 9 control mice underwent aortic perfusion with HIE, in which the standard dose elastase solution was heated to 100 °C for 30 min to eliminate enzymatic activity. HIE is the compound of reference used as a control for this model since it was described by Pyo et al. in 1998.[4] All experiments were performed with a single porcine pancreatic elastase (PPE) preparation derived from the same commercial source and lot.

Protocol

MRI was performed at day 0 before elastase perfusion, compared with optical grid measurement, and repeated 14 days after elastase perfusion. After MRI at day 14, a second laparotomy was performed, and the perfused segment of the abdominal aorta was reexposed and measured *in situ* before sacrifice. Pre-perfusion aortic diameter was measured before isolation of the abdominal aorta at the time of elastase perfusion, and post-perfusion aortic diameter was measured at least 5 min after successful restoration of arterial flow. Final aortic diameter measurements at day 14 were obtained *in vivo* immediately before euthanasia and approximately 1 h after MRI.

MRI

In vivo MRI was performed on a Bruker AVANCE 500 11.75 T (Bruker, Ettlingen, Germany) wide bore vertical imaging system equipped with microimaging gradients. Animals underwent isoflurane induction at 3%, and were inserted in a 30 mm diameter radiofrequency volume resonator. During the MRI acquisitions, 1.6–1.8% isoflurane in a 300 mL/min air-flow was administered through an adapted nose cone assuring a stable sleep under physiologic conditions. Breath-monitoring and gating were obtained using an SA Instruments (Stony Brook, NY, USA) system and a pressure sensor connected to an air-filled balloon. Temperature was maintained at 37 °C by heating of the surrounding magnetic field gradient coils. An angio FLASH sequence (TE = 2 ms, TR = 120 ms, flip angle 90°, FOV 30 mm, matrix 256 × 256, averages 2) was used to visualize the aorta in two longitudinal planes. These images served as a basis for perpendicular slice positioning of the vessel-wall imaging sequence (Fig. 1). For imaging the vessel wall, a respiratory-gated multi-slice spin-echo sequence was used with 9 slices, TR ~1500 ms, TE = 15 ms, FOV 20 mm, matrix size 256 × 256 μm,[2] slice thickness: 0.5 mm, interslice distance = 1 mm and a total duration of 12 min. Multi-slice FLASH imaging was then used to acquire positive-blood-contrast images from the same slices (TR = 60 ms, TE = 2.6 ms, flip angle = 30°, FOV = 20 mm, matrix size = 256 × 256, slice thickness = 0.5 mm, interslice distance = 1 mm). In order to obtain reproducible cranio-caudal slice positions between day 0 and 14, the lowermost slice was first placed at iliac bifurcation level, and the entire slice block was then shifted upward by 3 mm. The total duration of the protocol was 30 min.

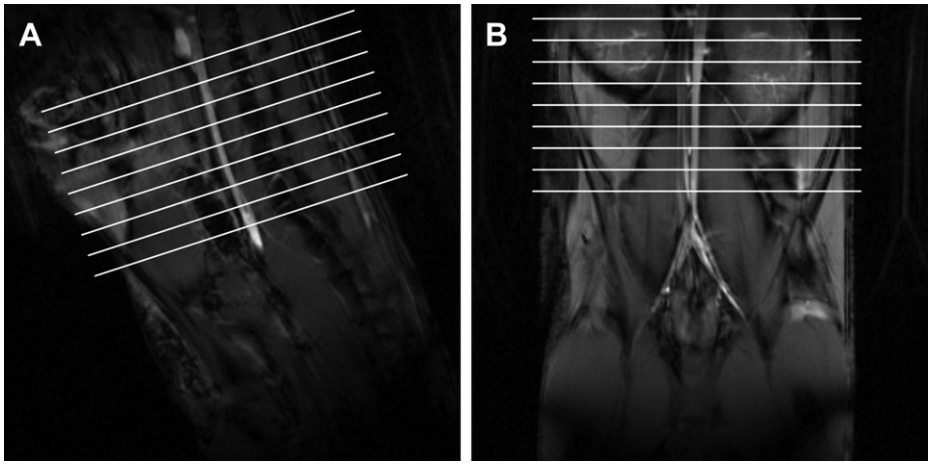

Figure 1. (A) Coronal and (B) sagittal abdominal FLASH angiography images used for perpendicular positioning of imaging slices.

Image analysis

MRI image analysis was performed using Image J 1.43u software by personnel blinded with respect to results from optic grid measurements. Measurements were repeated on two separate occasions using random selection of datasets and with operator blinding to prevent any bias.

Vessel diameters were calculated from strictly circular areas, which were manually fitted to the outer or inner contour of the vessel on the spin echo (black blood) images. The inner and outer vessel diameters were calculated from these circular areas. As an internal control, the aortic lumen diameter was also measured using the gradient echo images.

Aortic wall thickness was calculated by subtracting the inner from the outer area and the inner from the outer radius, both of which were measured on the spin-echo images. Among the 9 available slices, the one with the largest measured diameter was retained for comparison with the optic grid measurements, among which also the largest diameter was retained for comparison. In order to assess potential tissue structure changes between aneurysms and controls with MRI, aortic wall gray scale mean was calculated as the mean signal intensity on spin echo images using Image J 1.43u software and gray scale histogram function. The region of interest was delimited by the outer and inner contour of the vessel on the slice in which the diameter was the largest.

Statistics

Data are presented as group means ± SD or, if the data did not pass the normality test, as median with interquartile range. Student's *t* test was used to compare the means of two independent sample groups when values were sampled from Gaussian distribution. Otherwise the Mann–Whitney test was used. Mortality rates were compared with Fisher's exact test. Statistical analysis was performed with GraphPad PRISM version 3.00 for Windows 95 (GraphPad Software, San Diego, CA, USA). To assess the correlation between MRI and micro grid optic measurements, a linear regression analysis was performed. The Pearson coefficient was computed to measure the strength of the relation; P values ≤ 0.05 were considered significant. A Bland–Altman plot was used to compare the techniques.[16]

Results

With the four different elastase concentrations initially tested (0.1164 units/ml, 0.1455 units/ml, 0.1746 units/ml and 0.2328 units/ml) the final diameters obtained at 14 days were 0.95 ± 0.22, 1.12 ± 0.17, 1.10 ± 0.20, and 1.49 ± 0.48 mm, respectively, which were compared with the diameter obtained with HIE (0.92 ± 0.04 mm). We retained the concentration of 0.1455 units/ml for the MRI assessment, because it was the lowest elastase concentration producing a significant diameter increase compared with controls perfused with HIE ($P = 0.0112$). During these preparative experiments, mortality was 8.2%.

At day 0 of the main protocol, pre, per and post perfusion aortic diameters obtained with the optic grid during surgery did not differ significantly between groups, confirming that surgery protocol was comparable between the two groups (Table 1). There was an increase in aortic diameter right after perfusion in both groups. This is due to the initial perfusion of the aorta, which is performed under pressure. This perfusion over-expands the aorta, and when the pressure is released the aorta remains dilated. Perfusion creates the same initial diameter increase in both groups. The mortality rate in operated mice between day 0 and day 14 was 3 out of 18 mice (16%); this was not statistically different compared to the mortality observed in the first part of the experiment ($P = 0.3751$). MR image quality was such that morphologic measurements of the aorta were possible in all obtained images. A typical example of MRI images in both groups at day 0 and day 14 is shown in Fig. 2.

The mean aortic diameter measurements obtained with optic grid and MRI are shown in Table 2. At day 0, none of the measurements performed with optic grid or MRI were different between the groups. At day 14, aortic diameters obtained with the optic grid method were significantly higher in elastase-perfused mice than in controls, and a 100% increase in diameter from day 0 pre perfusion to day 14 was obtained in 6 out of 7 mice (85%) perfused initially with elastase, in agreement with a previous report using the elastase perfusion model.[17] Using MRI measurement we observed at day 14 a significantly larger outer aortic diameter in elastase-perfused mice compared to controls, in agreement with optic grid measurement. In addition, MRI allowed measuring the inner aortic diameter which was not available with optic grid measurement. The inner aortic

Table 1
Optic grid aortic diameter measurements immediately before (pre), during (per) and after (post) elastase or heat-inactivated elastase (HIE) perfusion.

Diameter (mm)	Elastase $N = 9$	HIE $N = 9$	P-value
Pre perfusion	0.533 ± 0.040	0.506 ± 0.032	NS
Per perfusion	0.964 ± 0.078	0.922 ± 0.042	NS
Post perfusion	0.823 ± 0.022	0.804 ± 0.016	NS

All data are given as means ± SEM. Statistical analyses were carried out using Student's *t*-test.

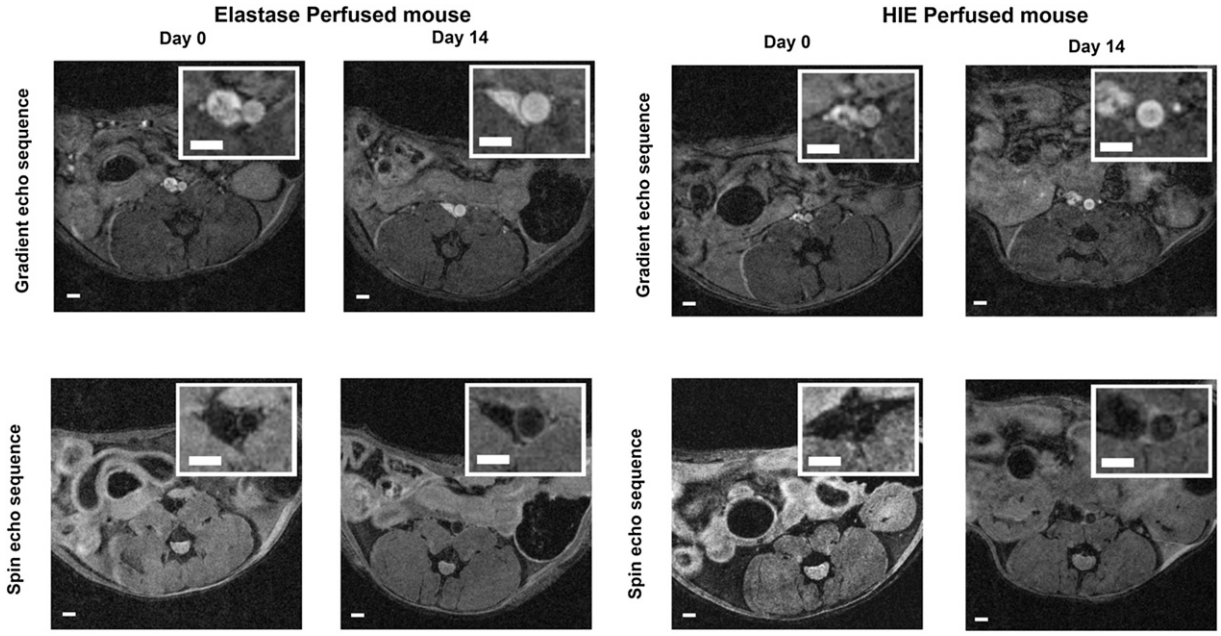

Figure 2. Typical example of MRI images in mice at day 0 and day 14 after elastase or heat-inactivated elastase perfusion. Scale bar = 1 mm.

diameter measurement was found to be significantly different between perfused mice and controls, on either spin echo images or gradient echo images. Overall, the most significant difference between the two groups was observed using the outer diameter assessed with the spin echo sequence.

There was a significant linear correlation ($P = 0.0001$) between MRI and optic measurements of the outer diameter at day 0 and day 14, with both groups pooled (Fig. 3). Bland–Altman analyses of MRI and optic grid measurements showed good agreement between the two methods in day 0 mice, day 14 controls and day 14 elastase-perfused mice. At day 0, MRI showed significantly higher aortic diameter values, and with increasing diameters at day 14 the bias was reduced by one half (Fig. 4). Diameters obtained with gradient echo images were higher, which is likely due to a relatively high signal intensity from the blood and blurring. MRI also allowed us to measure aortic wall thickness. At day 14, wall thickness was significantly greater in elastase-perfused mice compared with controls. Both groups showed a significant increase in aortic wall thickness from day 0 to day 14 (Fig. 5). The analysis of the gray scale value between aortas perfused with HIE and aortas perfused with elastase at day 14 did not show any difference (Fig. 6).

Discussion

In vivo imaging technologies are of obvious interest in the study of animal models of AAA. To the best of our knowledge, this is the first study demonstrating the feasibility of *in vivo* aortic measurements in the elastase-induced aneurysm mouse model. We have also showed that significant diameter differences between elastase-perfused mice and HIE-perfused mice can be revealed using MRI at 14 days, and this finding was in agreement with the ocular grid reference technique[4] carried out on the same animals. With an acceptable mortality rate, a high level of reproducibility and the possibility to perform longitudinal studies, this approach offers a significant benefit in terms of animal sacrifice, since in future studies the kinetics of the aortic diameter might be assessed with MRI at several time points, following up animals individually instead of sacrificing the animals at each stage for comparison purposes. Beyond diameter measurements we also demonstrated the ability to assess aortic wall thickness non-invasively, which offers further possibilities for the analysis of aneurysm walls. The same measurements are obviously possible in transgenic animals.

The ability to perform non-invasive follow-up and aortic wall analysis in different AAA animal models[13,18] with the same imaging modality now enables comparison of different complementary models and studies of the pathologic processes leading to aneurysm development.

In this specific model, the relatively small size of the aortic aneurysm is one of the major difficulties when using non-invasive measurements. In 1998, Fayad et al.[9] demonstrated the first *in vivo* MR microscopy images of the arterial wall of wild type and genetically engineered mice, such as ApoE-KO mice, that non-

Table 2
Comparison of aortic diameter measured with MRI and optic grid at day 0 and day 14.

	Day 0			Day 14		
	HIE $N = 9$	Elastase $N = 9$	P value	HIE $N = 8$	Elastase $N = 7$	P value
MRI – spin echo						
Inner diameter (mm)	0.525 ± 0.022	0.564 ± 0.067	0.1457	0.799 ± 0.057	0.865 ± 0.051	0.0335
Outer diameter (mm)	0.745 ± 0.035	0.773 ± 0.064	0.2988	1.070 ± 0.048	1.203 ± 0.105	0.0067
MRI – gradient echo						
Inner diameter (mm)	0.681 ± 0.035	0.720 ± 0.067	0.1966	0.851 ± 0.027	0.927 ± 0.056	0.0078
Optic grid						
Outer diameter (mm)	0.506 ± 0.032	0.533 ± 0.040	0.1672	0.939 ± 0.070	1.150 ± 0.153	0.0038

Mean ± SEM aortic diameter value obtained with MRI and optic measurement.
HIE: heat-inactivated elastase.

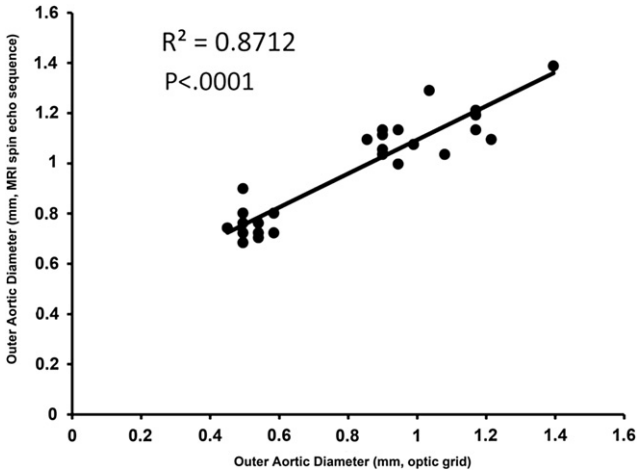

Figure 3. Comparison of outer aortic diameters as measured by MRI or optic grid at day 0 and day 14 for both groups ($n = 33$ measurements). The linear regression yielded a significant positive correlation.

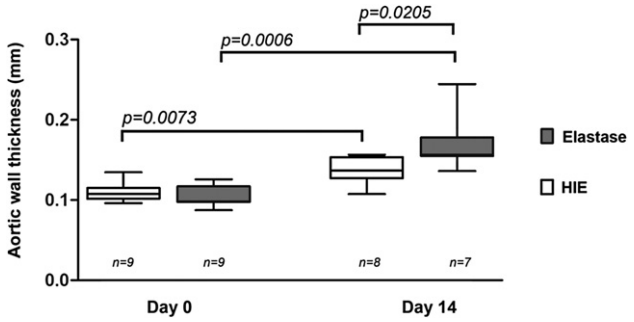

Figure 5. Box and whisker plot of aortic wall thickness. Box represents median and interquartile range and whiskers the extreme values. Comparison of aortic wall thickness at day 0 and day 14 between control and elastase-perfused mice as measured by spin echo MRI.

invasively identified and characterized atherosclerotic lesion burden. It was shown later that these measurements were also possible at early stages of plaque development.[10] These studies demonstrated the potential of high resolution MRI in this field.

In a more recent study, Turner et al.[18] had to deal with larger aneurysms compared to the AAA elastase-induced model, since the study was carried out on the AngII ApoE-KO model of aneurysm. In this model, the AAA area reached 4 mm^2 after 4 weeks, which is equivalent to a diameter of 2.26 mm, and this facilitated an assessment with MRI.[18] In this particular study, it is interesting to note that the AAA area increased very significantly while in the same period of time the aortic lumen area decreased. This phenomenon was not observed in our study, in which a parallel increase of the lumen and of the aorta was observed as shown in Table 2.

Several studies have used duplex ultrasound and have shown reliable results with the AngII ApoE-KO model.[19,20] However, in highly dilated aortas, some difficulties appear in sharply delineating the lumen from the aortic wall boundary in grossly diseased vessels with this technique. The AAAs obtained with the elastase perfusion model are relatively small compared to the AngII ApoE-KO model despite a relatively smooth aortic wall boundary. The aortic wall thickness is probably difficult to reliably measure with ultrasound, partly due to the aortic position behind the guts in the abdomen. In a recent report, Azuma et al. have validated high-frequency ultrasound imaging to non-invasively assess AAA development in the murine model of elastase-induced AAA.[21] This study, however, was entirely based on aortic lumen measurements, which is likely related to the aforementioned difficulties in delineating the external boundaries of the aneurysm with ultrasound.[19,20] Taken together, these data show that the assessment of aortic wall thickness in two of the main AAA mice models seems to be challenging with ultrasound. However, aortic wall visualization with ultrasound might become important in aneurysm research given the recent developments in contrast-enhanced ultrasound, which can assess neovascularization in the vessel wall and probe aortic wall biology with microbubbles targeted to specific vascular endothelial cell ligands.[22]

In a previous study, it was demonstrated that small aortic wall thicknesses are measurable with MRI in ApoE-KO mice.[10] In this study, we were able to reproduce these measurements at the level of the abdominal aorta in the elastase perfusion model. Moreover, we were able to show that aortic wall thickness increases when perfusion is performed with elastase rather than HIE. We observed that in spin echo images the aortic wall is particularly well visualized at the level of the inter aorto-caval space, because the aorta is surrounded by arterial and venous blood. This isolated part of the aorta might be a useful target for advanced MRI analyses of the aortic wall. In human aneurysms, it has been reported that localized wall thickness is a possible important feature of AAAs.[23] The ability to assess this parameter with MRI in the elastase mouse model may therefore enable new experimental research on this particular aneurysm feature.

This study is in agreement with recent non-invasive measurements of AAA using ultrasound or MRI in un-operated aorta that showed larger diameters than those monitored by visual microscopy.[20,21,24] Different hypotheses have been presented to explain this finding.[21] We hypothesize that vascular tone plays a major role.[25] Interestingly, we observed a smaller bias in the HIE group at day 14 compared to day 0. The aortic dilatation performed at day 0 with HIE during the procedure probably modifies slightly the ability of the aorta to respond to external vasoactive stimuli.

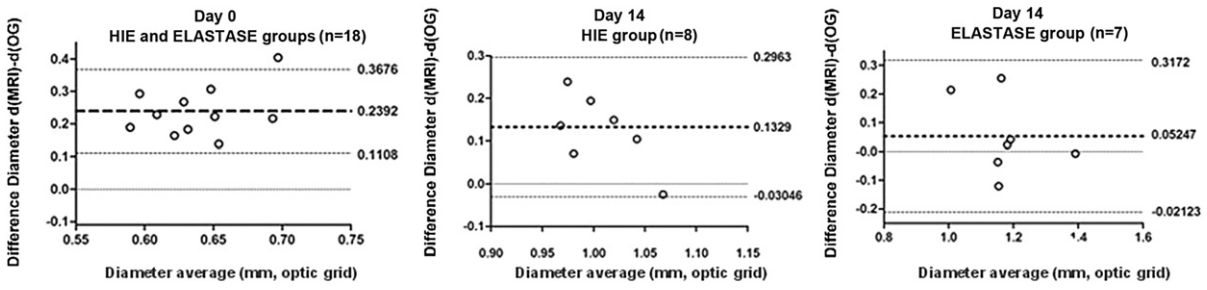

Figure 4. Bland–Altman analyses comparing MRI and optic grid measurements of aortic diameter in mice at day 0 (both groups), in mice at day 14 after HIE and in mice at day 14 after elastase perfusion.

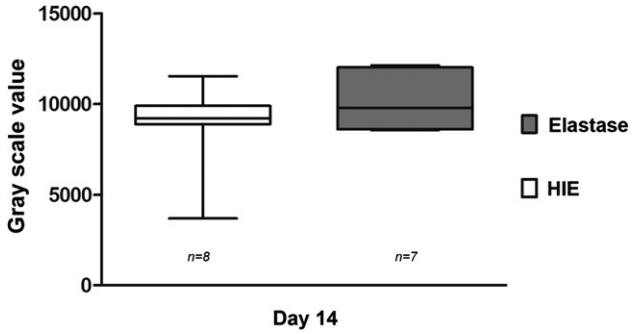

Figure 6. Box and whisker plot of gray scale value measured on aortic wall with MRI at day 14 in HIE-perfused mice and elastase-perfused mice. Box represents median and interquartile range and whiskers the extreme values ($P = 3357$).

Moreover, the bias was smallest at day 14 in the aorta perfused with elastase. At this stage, the elastic layer was more severely injured due to fragmentation of elastin layers and compensatory collagen accumulation. MRI, however, allowed detection of diameter differences between HIE and elastase perfused mice at day 14.

The ability to assess the aortic wall with MRI in the elastase aneurysm mouse model offers interesting perspectives for studying this pathology. The different surgical therapies for AAA are characterized by their individual mortality pattern. In the interest of benefit for the patient, surgical management of AAA is therefore commonly indicated only when the aneurysm reaches a diameter greater than 55 mm.[26] Below this diameter, simple close follow-up is recommended. However, during this period the risk of aneurysm rupture remains. To date, the most reliable parameter correlating with the risk of rupture is the AAA diameter. Thus, it is of interest to create a model of aneurysm follow-up and to establish new markers of rapid evolution or risk of rupture during this follow-up period. This approach will also help to assess the efficacy of future medical therapies on the stabilization of the AAA growth. Moreover, it has been shown that MRI provides the possibility to use ultra-small superparamagnetic iron oxide (USPIO) to detect the acute inflammatory process involved in the development of the AngII ApoE-KO model.[27] In a second step, it has been demonstrated that uptake of USPIO in human AAA identifies cellular inflammation and appears to distinguish those patients with more rapidly progressive AAA expansion.[28] Recently, Klink and colleagues demonstrated in a new AAA mouse model that high-resolution, multisequence MRI allowed for longitudinal monitoring of AAA progression while the presence of collagen was visualized by nanoparticle-enhanced MRI.[11] Taken together, these data suggest that mouse models give complementary information useful for the determination of new biomarkers for aneurysm development.

One of the main clinical goals of this study was to identify new imaging markers of AAA evolution. These markers will have numerous potential clinical applications also in the EVAR field, such as evaluation of aortic wall changes after EVAR performed with a nitinol stent graft and assessment of the neck quality before EVAR.

Conclusion

High-resolution MRI in mice may provide information about the progression of cardiovascular disease by characterizing the size, the scope and the biochemical structure of the aortic wall. These results show the feasibility of morphologic measurements of aneurysms after aortic elastase perfusion in mice using MRI. The results correlated well with optical measurements. Moreover, MRI offers the possibility to assess the aortic wall thickness *in vivo*, which is not possible with optic grid measurements. This approach combined with a wider range of mouse models of aneurysm might contribute to a better understanding of the pathologic mechanisms that contribute to aneurysmal degeneration and to the development of new therapeutic approaches.

Funding

This study was funded by grants from “Société de Chirurgie Vasculaire Française” (2007 and 2009) and a grant from CNRS (UMR 7339).

Conflict of Interest

None.

References

1 Daugherty A, Cassis LA. Mouse models of abdominal aortic aneurysms. *Arterioscler Thromb Vasc Biol* 2004;**24**(3):429–34.
2 Longo GM, Xiong W, Greiner TC, Zhao Y, Fiotti N, Baxter BT. Matrix metalloproteinases 2 and 9 work in concert to produce aortic aneurysms. *J Clin Invest* 2002;**110**(5):625–32.
3 Daugherty A, Manning MW, Cassis LA. Angiotensin II promotes atherosclerotic lesions and aneurysms in apolipoprotein E-deficient mice. *J Clin Invest* 2000;**105**(11):1605–12.
4 Pyo R, Lee JK, Shipley JM, Curci JA, Mao D, Ziporin SJ, et al. Targeted gene disruption of matrix metalloproteinase-9 (gelatinase B) suppresses development of experimental abdominal aortic aneurysms. *J Clin Invest* 2000;**105**(11):1641–9.
5 Saraff K, Babamusta F, Cassis LA, Daugherty A. Aortic dissection precedes formation of aneurysms and atherosclerosis in angiotensin II-infused, apolipoprotein E-deficient mice. *Arterioscler Thromb Vasc Biol* 2003;**23**(9):1621–6.
6 Manning MW, Cassi LA, Huang J, Szilvassy SJ, Daugherty A. Abdominal aortic aneurysms: fresh insights from a novel animal model of the disease. *Vasc Med* 2002;**7**(1):45–54.
7 Anidjar S, Salzmann JL, Gentric D, Lagneau P, Camilleri JP, Michel JB. Elastase-induced experimental aneurysms in rats. *Circulation* 1990;**82**(3):973–81.
8 Wassef M, Baxter BT, Chisholm RL, Dalman RL, Fillinger MF, Heinecke J, et al. Pathogenesis of abdominal aortic aneurysms: a multidisciplinary research program supported by the National Heart, Lung, and Blood Institute. *J Vasc Surg* 2001;**34**(4):730–8.
9 Fayad ZA, Fallon JT, Shinnar M, Wehrli S, Dansky HM, Poon M, et al. Noninvasive *in vivo* high-resolution magnetic resonance imaging of atherosclerotic lesions in genetically engineered mice. *Circulation* 1998;**98**(15):1541–7.
10 Kober F, Canault M, Peiretti F, Mueller C, Kopp F, Alessi MC, et al. MRI follow-up of TNF-dependent differential progression of atherosclerotic wall-thickening in mouse aortic arch from early to advanced stages. *Atherosclerosis* 2007;**195**(2):e93–9.
11 Klink A, Heynens J, Herranz B, Lobatto ME, Arias T, Sanders HM, et al. *In vivo* characterization of a new abdominal aortic aneurysm mouse model with conventional and molecular magnetic resonance imaging. *J Am Coll Cardiol* 2011;**58**(24):2522–30.
12 McFadden EP, Chaabane L, Contard F, Guerrier D, Briguet A, Douek P, et al. *In vivo* magnetic resonance imaging of large spontaneous aortic aneurysms in old apolipoprotein E-deficient mice. *Invest Radiol* 2004;**39**(10):585–90.
13 Deux JF, Dai J, Riviere C, Gazeau F, Meric P, Gillet B, et al. Aortic aneurysms in a rat model: *in vivo* MR imaging of endovascular cell therapy. *Radiology* 2008;**246**(1):185–92.
14 Bartoli MA, Parodi FE, Chu J, Pagano MB, Mao D, Baxter BT, et al. Localized administration of doxycycline suppresses aortic dilatation in an experimental mouse model of abdominal aortic aneurysm. *Ann Vasc Surg* 2006;**20**(2):228–36.
15 Pagano MB, Bartoli MA, Ennis TL, Mao D, Simmons PM, Thompson RW, et al. Critical role of dipeptidyl peptidase I in neutrophil recruitment during the development of experimental abdominal aortic aneurysms. *Proc Natl Acad Sci U S A* 2007;**104**(8):2855–60.
16 Bland JM, Altman DG. Statistical methods for assessing agreement between two methods of clinical measurement. *Lancet* 1986;**1**(8476):307–10.
17 Bergoeing MP, Arif B, Hackmann AE, Ennis TL, Thompson RW, Curci JA. Cigarette smoking increases aortic dilatation without affecting matrix metalloproteinase-9 and -12 expression in a modified mouse model of aneurysm formation. *J Vasc Surg* 2007;**45**(6):1217–27.
18 Turner GH, Olzinski AR, Bernard RE, Aravindhan K, Karr HW, Mirabile RC, et al. *In vivo* serial assessment of aortic aneurysm formation in apolipoprotein E-deficient mice via MRI. *Circ Cardiovasc Imaging* 2008;**1**(3):220–6.
19 Barisione C, Charnigo R, Howatt DA, Moorleghen JJ, Rateri DL, Daugherty A. Rapid dilation of the abdominal aorta during infusion of angiotensin II detected by noninvasive high-frequency ultrasonography. *J Vasc Surg* 2006;**44**(2):372–6.
20 Martin-McNulty B, Vincelette J, Vergona R, Sullivan ME, Wang YX. Noninvasive measurement of abdominal aortic aneurysms in intact mice by a high-frequency ultrasound imaging system. *Ultrasound Med Biol* 2005;**31**(6):745–9.

21 Azuma J, Maegdefessel L, Kitagawa T, Dalman RL, McConnell MV, Tsao PS. Assessment of elastase-induced murine abdominal aortic aneurysms: comparison of ultrasound imaging with in situ video microscopy. *J Biomed Biotechnol* 2011;**2011**:252141.
22 Shalhoub J, Owen DR, Gauthier T, Monaco C, Leen EL, Davies AH. The use of contrast enhanced ultrasound in carotid arterial disease. *Eur J Vasc Endovasc Surg* 2010;**39**(4):381–7.
23 Vorp DA, Lee PC, Wang DH, Makaroun MS, Nemoto EM, Ogawa S, et al. Association of intraluminal thrombus in abdominal aortic aneurysm with local hypoxia and wall weakening. *J Vasc Surg* 2001;**34**(2):291–9.
24 Knipp BS, Ailawadi G, Sullivan VV, Roelofs KJ, Henke PK, Stanley JC, et al. Ultrasound measurement of aortic diameters in rodent models of aneurysm disease. *J Surg Res* 2003;**112**(1):97–101.
25 Janssen BJ, De Celle T, Debets JJ, Brouns AE, Callahan MF, Smith TL. Effects of anesthetics on systemic hemodynamics in mice. *Am J Physiol Heart Circ Physiol* 2004;**287**(4):H1618–24.
26 Moll FL, Powell JT, Fraedrich G, Verzini F, Haulon S, Waltham M, et al. Management of abdominal aortic aneurysms clinical practice guidelines of the European society for vascular surgery. *Eur J Vasc Endovasc Surg* 2011;**41**(Suppl. 1):S1–58.
27 Turner GH, Olzinski AR, Bernard RE, Aravindhan K, Boyle RJ, Newman MJ, et al. Assessment of macrophage infiltration in a murine model of abdominal aortic aneurysm. *J Magn Reson Imaging* 2009;**30**(2):455–60.
28 Richards JM, Semple SI, MacGillivray TJ, Gray C, Langrish JP, Williams M, et al. Abdominal aortic aneurysm growth predicted by uptake of ultrasmall superparamagnetic particles of iron oxide: a pilot study. *Circ Cardiovasc Imaging* 2011;**4**(3):274–81.